

Power-law dependence on frequency of the Raman-scattering intensity of percolating networks

Takamichi Terao and Tsuneyoshi Nakayama

Department of Applied Physics, Hokkaido University, Sapporo 060, Japan

(Received 27 September 1995)

Large-scale simulations have been carried out for elucidating the power-law dependence on frequency of the Raman-scattering intensity $I_{\alpha\beta}(\omega)$ for $d=3$ bond-percolating networks. We have used for this purpose a simple but powerful and accurate numerical method. Taking into account the dipole-induced-dipole mechanism, the clear evidence of the power-law dependence on frequency for $I_{\alpha\beta}(\omega)$ has been obtained above and below the phonon-fracton crossover frequency ω_c . In addition, the profiles of the ω dependence for dynamical structure factor $S(\mathbf{q},\omega)$ for $d=3$ percolating networks are given for networks above the percolation threshold p_c . Physical interpretations for these results are given in a line with the dynamic scaling argument.

Scattering experiments are crucial for understanding dynamical properties of complex systems.¹ In particular, scattering experiments on fractal or percolating networks have revealed peculiar properties of vibrational excitations called fractons.^{2,3} Tsujimi *et al.*⁴ have performed Raman-scattering experiments for silica aerogels and found the power-law dependence on frequency of the Raman-scattering intensity. This is clear evidence of the ω dependence of $I_{\alpha\beta}(\omega)$ for fractal structures. To analyze the data, they used ensemble averaged wave functions for fractons. It has been pointed out that the use of ensemble averaged wave functions are not appropriate for the calculation of scattering matrix elements.⁵ Alexander, Courtens, and Vacher⁶ have proposed a scaling theory for the dynamical structure factor $S(q,\omega)$ and the inelastic light scattering intensity $I_{\alpha\beta}(\omega)$ on percolating networks, assuming the validity of single-length scaling postulate (SLSP). The validity of the SLSP has been confirmed by numerical calculations^{7,8} for $d=2$ and $d=3$ percolating networks at the percolation threshold p_c , where the system is considered to be self-similar at any length scale. Montagna *et al.*⁹ and Mazzacurati *et al.*¹⁰ have numerically studied the Raman-scattering intensity for site-percolating networks. Most of these have used direct diagonalization techniques (except Ref. 8), which consumes a large amount of memory sizes. As a result, the numbers of sites are limited within the order of 10^3-10^4 , the system size up to $L \leq 29$ for $d=3$, which cause the sample dependence or the finite-size effect on the results. Due to this difficulty, no clear evidence has been given on the power-law dependence on frequency above and below the phonon-fracton crossover frequency ω_c . The development of a numerical method for calculating the dynamic correlation function of large systems has been highly required in order to obtain the correct insight into the dynamic correlation functions such as $I_{\alpha\beta}(\omega)$ or $S(\mathbf{q},\omega)$.

This paper, at first, presents an efficient numerical method to calculate the dynamic correlation function for very large systems. Our algorithm, based on the forced oscillator method,¹¹⁻¹⁴ can treat very large systems of the order of 10^6 using a computer with 64 Mbyte memory space. These large sizes enable us to obtain the definite informations of dynamic correlation functions with arbitrary resolution of frequency $\delta\omega$ without performing sample-average procedure. We apply our algorithm to investigate the power-law dependence on

frequency of the Raman-scattering intensities $I_{\alpha\beta}(\omega)$ [$(\alpha,\beta) = (x,x), (x,y)$] for $d=3$ bond-percolating networks. In real materials such as aerogels, the systems above the percolation threshold p_c are relevant, so we pay attention to these quantities for the systems above p_c .

Let us consider the equation of motion for vibrational systems with the external force on each site. This is given by

$$m_\kappa \ddot{u}_{\kappa l}^\alpha(t) = \sum_{\kappa' l' \beta} \phi_{\kappa l, \kappa' l'}^{\alpha\beta} u_{\kappa' l'}^\beta(t) + F_{\kappa l}^\alpha \cos(\Omega t), \quad (1)$$

where $u_{\kappa l}^\alpha(t)$ is the displacement at the atom κ of the cell l with the Cartesian component $\alpha (=x, y, z)$, $\phi_{\kappa l, \kappa' l'}^{\alpha\beta}$ the force constant between the atom (κ, l) and (κ', l') , $F_{\kappa l}^\alpha$ and Ω are the amplitude and the frequency of the external force, respectively.

The energy $E(\Omega, t)$ of the system after t time under the initial conditions $u_{\kappa l}^\alpha(t=0) = \dot{u}_{\kappa l}^\alpha(t=0) = 0$ becomes

$$E(\Omega, t) = \frac{1}{2} \sum_\lambda \frac{\sin^2\{(\Omega - \omega_\lambda)t/2\}}{(\Omega - \omega_\lambda)^2} \left\{ \sum_{\kappa l \alpha} F_{\kappa l}^\alpha e_{\kappa l}^\alpha(\lambda) \right\}^2, \quad (2)$$

where ω_λ is the eigenfrequency of the mode λ , and $e_{\kappa l}^\alpha(\lambda)$ the α component of the eigenvector $\mathbf{e}_{\kappa l}(\lambda) \equiv [e_{\kappa l}^x(\lambda), e_{\kappa l}^y(\lambda), e_{\kappa l}^z(\lambda)]$ at the atom κ of the cell l , respectively.^{11,13,14} For sufficiently large $t=T$, $E(\Omega, T)$ becomes

$$E(\Omega, T) \approx \frac{\pi T}{4} \sum_\lambda \delta(\Omega - \omega_\lambda) \left\{ \sum_{\kappa l \alpha} F_{\kappa l}^\alpha e_{\kappa l}^\alpha(\lambda) \right\}^2. \quad (3)$$

We should note that the right-hand side of Eq. (3) is related to the definition of the Raman-scattering intensity $I_{\alpha\beta}(\omega)$, which is written by

$$I_{\alpha\beta}(\omega) \equiv \frac{1}{2\pi N} \int dt e^{i\omega t} \sum_{mn} \langle \mu_{\alpha\beta}^m(t) \mu_{\alpha\beta}^n(0) \rangle, \quad (4)$$

where $\langle \dots \rangle$ is the thermal average, N the number of sites, and $\mu_{\alpha\beta}^n(t)$ the polarizability at the site $n \equiv (\kappa, l)$, respectively. Neglecting the contribution from elastic scattering, one has

$$I_{\alpha\beta}(\omega) = \frac{\hbar}{2N^2} \frac{\langle n+1 \rangle}{\omega} \sum_{\lambda} \delta(\omega - \omega_{\lambda}) \left\{ \sum_{n\gamma} f_{n\gamma} e_{n\gamma}(\lambda) \right\}^2, \quad (5)$$

where $\langle n+1 \rangle$ is the Bose factor expressed by $1/(1-e^{-\beta\omega})$, and $f_{n\gamma} \equiv \sum_m \partial \mu_{\alpha\beta}^m / \partial u_{n\gamma}$. Taking into account the dipole-induced-dipole (DID) mechanism, one can express $f_{n\gamma}$ in Eq. (5) using the derivative of the dipole propagator^{7,9,10} as

$$f_{n\gamma} \equiv \sum_m \tilde{\mu}_m \tilde{\mu}_n \left[-3 \frac{\delta_{\alpha\beta} r_{\gamma} + \delta_{\beta\gamma} r_{\alpha} + \delta_{\gamma\alpha} r_{\beta}}{r^5} + 15 \frac{r_{\alpha} r_{\beta} r_{\gamma}}{r^7} \right], \quad (6)$$

where r_{α} is defined as $\mathbf{r}_{mn} \equiv \mathbf{R}_m - \mathbf{R}_n = (r_x, r_y, r_z)$, $r \equiv |\mathbf{r}_{mn}|$, and $\tilde{\mu}_n$ the bare polarizability of site n , respectively. The value of $\tilde{\mu}_n$ is given by

$$\tilde{\mu}_n = \begin{cases} 1 & ; \text{occupied,} \\ 0 & ; \text{unoccupied.} \end{cases} \quad (7)$$

Here the bare polarizability at each site is taken to be isotropic. Using Eqs. (3) and (5), the Raman-scattering intensity is expressed as

$$I_{\alpha\beta}(\omega) \approx \frac{\hbar}{2N^2} \frac{\langle n+1 \rangle}{\omega} \frac{4E(\omega, T)}{\pi T}, \quad (8)$$

where the amplitude of the periodic force $\{F_{\kappa l}^{\alpha}\}$ in Eq. (8) should be taken as $F_{\kappa l}^{\alpha} \equiv f_{n\alpha}$. This method enables us to calculate Eq. (5) with arbitrary resolution of frequency $\delta\omega$ by choosing the proper time interval $T \approx 4\pi/\delta\omega$.¹³

We use the above algorithm for the calculation of $I_{\alpha\beta}(\omega)$ for bond-percolating networks. There exists the characteristic length scale called the *correlation length* $\xi \propto |p - p_c|^{-\nu}$ in this system, where p is the percolation concentration and p_c is the percolation threshold. At larger length scale than ξ , the system is considered to be homogeneous. While at shorter length scale than ξ , the self-similarity becomes relevant. There is a crossover frequency ω_c related to ξ as $\omega_c \propto \xi^{-D_f/\tilde{d}}$, where D_f is the fractal dimension and \tilde{d} is called spectral dimension.³ The value of \tilde{d} is known to be close to $\frac{4}{3}$ for percolating networks at any Euclidean dimension $d(\geq 2)$.^{2,3} At lower frequencies $\omega < \omega_c$, vibrational excitations are conventional (weakly localized) phonons. At higher frequencies $\omega > \omega_c$, excitations are *strongly* localized and called fractons. In the following, we consider scalar displacements with one atom in a unit cell and the unit mass ($m_{\kappa} = 1$). The matrix elements ϕ_{mn} in Eq. (1) are taken as

$$\phi_{mn} = \begin{cases} z_m & : m = n \\ -1 & : \text{nearest neighbor interaction} \\ 0 & : \text{otherwise,} \end{cases} \quad (9)$$

where z_m is the coordination number at the site m . We show in Fig. 1 the normalized density of states (DOS) for $d=3$ bond-percolating network formed on a simple-cubic lattice with the percolation concentration $p=0.31$ ($> p_c=0.25$). The system size is $L=120$ and the number of sites is 1 302 424. The periodic boundary condition is taken for calculations. The crossover frequency ω_c of this system is estimated from

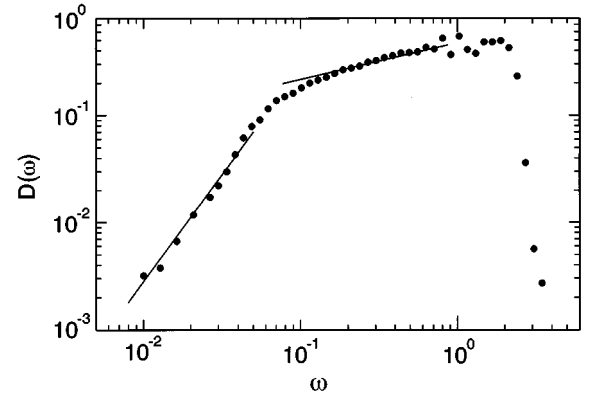


FIG. 1. The ω dependence of the normalized density of states $\mathcal{D}(\omega)$ of $d=3$ bond-percolating network at $p=0.31$ ($> p_c=0.249$) formed on $120 \times 120 \times 120$ cubic lattice.

Fig. 1 as $\omega_c \approx 0.07$. The calculated DOS clearly follows the Debye density of states $\mathcal{D}(\omega) \propto \omega^2$ for $\omega < \omega_c$, while the DOS obeys $\mathcal{D}(\omega) \propto \omega^{\tilde{d}-1}$ ($\tilde{d} \approx 4/3$) for $\omega > \omega_c$.

We have calculated the Raman-scattering intensities for $d=3$ bond-percolating networks formed on a simple-cubic lattice, taking into account the dipole-induced-dipole mechanism.^{6,7,9,10} The Raman-scattering intensity $I_{\alpha\beta}(\omega)$ can be expressed as^{1,3}

$$I_{\alpha\beta}(\omega) = \frac{\langle n+1 \rangle}{\omega} \mathcal{D}(\omega) C_{\alpha\beta}(\omega), \quad (10)$$

where $\mathcal{D}(\omega)$ is the DOS and $C_{\alpha\beta}(\omega)$ is the Raman-coupling coefficient. Alexander, Courtens, and Vacher⁶ have given the scaling argument for the Raman coupling coefficient for percolating networks and predicted the following power-law dependence,

$$C(\omega) \propto \omega^{2\tilde{d}(\sigma+d)/D_f - 3\tilde{d}}, \quad (11)$$

where D_f is the fractal dimension and σ is the exponent for strain. They have suggested that the value of $\sigma(\geq 1)$ should be not much larger than unity. Numerical studies by Stoll, Kolb, and Courtens⁷ and Nakayama and Yakubo⁸ have confirmed the validity of this scaling prediction. Figure 2(a) shows the reduced Raman-scattering intensity $I_{\alpha\beta}(\omega)/\langle n+1 \rangle$ as a function of frequency ω at the percolation threshold ($p=p_c=0.249$). The ordinate of Fig. 2(a) presents the reduced Raman intensity with arbitrary units. The system size is $L=120$ and the number of sites is 264,311. Solid circles and solid squares in Fig. 2(a) represent the calculated results for the polarized scattering $[(\alpha, \beta) = (x, x)]$ and for the depolarized scattering $[(\alpha, \beta) = (x, y)]$, respectively. We clearly see the power-law dependence $I_{xx}(\omega)/\langle n+1 \rangle \propto \omega^{-0.44 \pm 0.05}$ and $I_{xy}(\omega)/\langle n+1 \rangle \propto \omega^{-0.46 \pm 0.05}$ in much wider frequency band compared with previous studies.^{7,9,10} The use of Eq. (10) and the fracton DOS $\mathcal{D}(\omega) \propto \omega^{1/3}$ leads to the power-law dependence of the Raman-coupling coefficients $C_{xx}(\omega) \propto \omega^{0.23 \pm 0.05}$ and $C_{xy}(\omega) \propto \omega^{0.21 \pm 0.05}$ in the fracton regime. The value of the exponent σ in Eq. (11) is obtained from these results as close to unity, namely, $\sigma = 0.97 \pm 0.05$. Figure 2(b) gives the reduced Raman intensity $I_{xx}(\omega)/\langle n+1 \rangle$ for the $d=3$ bond-percolating network at $p=0.31$ ($> p_c=0.249$). The intensity in Fig. 2(b) is smaller than those in Fig. 2(a). This is because

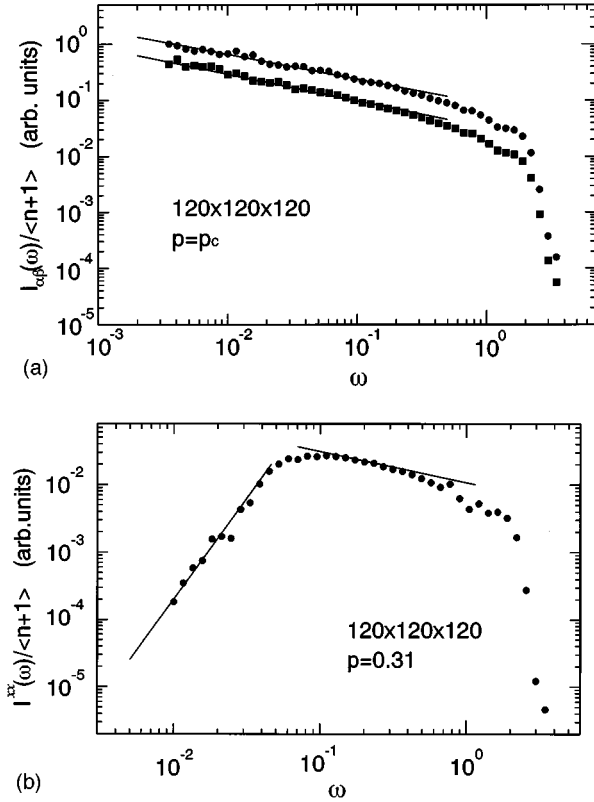


FIG. 2. (a) The ω dependence of the reduced Raman intensity $I_{\alpha\beta}(\omega)/\langle n+1 \rangle$ of the $d=3$ bond-percolating network at $p=p_c (=0.249)$ formed on a $120 \times 120 \times 120$ cubic lattice. Solid circles and squares represent the calculated results for the polarized scattering $[(\alpha, \beta) = (x, x)]$ and the depolarized scattering $[(\alpha, \beta) = (x, y)]$, respectively. (b) The ω dependence of the reduced Raman intensity $I_{xx}(\omega)/\langle n+1 \rangle$ of the $d=3$ bond-percolating network at $p=0.31$ formed on a $120 \times 120 \times 120$ cubic lattice.

the system at p_c [Fig. 2(a)] is much diluted in comparison with the case above p_c .¹⁰ The drastic change of the ω dependence of the reduced Raman intensity is observed at the phonon-fracton crossover frequency $\omega_c \approx 0.07$. The calculated ω dependence of the reduced Raman intensity $I_{xx}(\omega)/\langle n+1 \rangle$ is proportional to ω^3 for $\omega < \omega_c$, indicating phonon contribution. Note that the substitution of the phonon density of states $\mathcal{D}(\omega) \propto \omega^2$ and the Raman-coupling coefficient $C_{xx}(\omega) \propto \omega^2$ for phonons into Eq. (8) recovers the calculated frequency dependence for $I_{xx}(\omega) \propto \omega^3$. For $\omega > \omega_c$, the calculated results show that $I_{xx}(\omega)/\langle n+1 \rangle$ is proportional to $\omega^{-0.44}$, which has the same power-law dependence as solid circles given in Fig. 2(a), indicating the contribution from fractons. We have shown in Fig. 2(b) the clear evidence of the power-law dependence of the Raman intensity above and below the phonon-fracton crossover frequency ω_c . We should stress that the Raman intensity in the frequency regime $\omega > \omega_c$ takes the same ω dependence as that for the system at the percolation threshold p_c . The sample-average procedure is not taken due to the large number of sites in our system in these calculations.

Finally, let us show the calculated results of dynamical structure factors using the formula Eq. (3). The dynamical structure factor $S(\mathbf{q}, \omega)$ is defined as^{13,15}

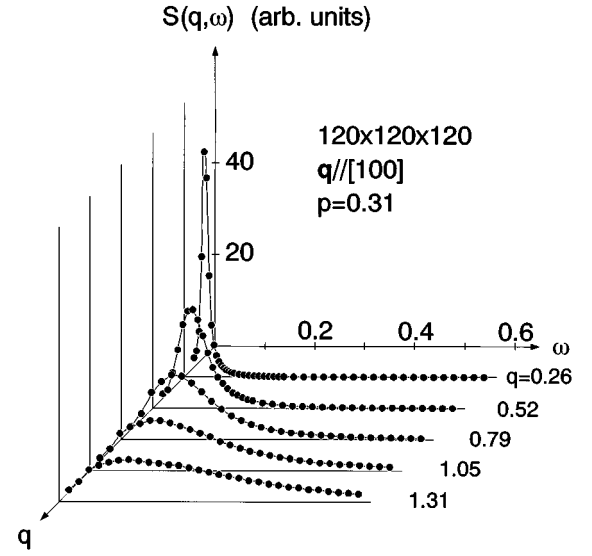


FIG. 3. The ω dependence of the dynamical structure factor $S(\mathbf{q}, \omega)$ of the $d=3$ bond-percolating network at $p=0.31$ formed on a $120 \times 120 \times 120$ cubic lattice.

$$S(\mathbf{q}, \omega) \equiv \frac{\langle n+1 \rangle}{\omega N} \sum_{\lambda} \delta(\omega - \omega_{\lambda}) \left| \sum_{\kappa l} \{ \mathbf{q} \cdot \mathbf{e}_{\kappa l}(\lambda) \} e^{-i\mathbf{q} \cdot \mathbf{R}_{\kappa l}} \right|^2 \quad (12)$$

where \mathbf{q} is the wave vector, and $\mathbf{R}_{\kappa l}$ the positional vector of the atom κ of the cell l , respectively. Putting the following two sets of $\{F_{\kappa l}^{\alpha}\}$ into Eq. (1),

$$F_{\kappa l}^{\alpha}(c) = q_{\alpha} F_0 \cos(\mathbf{q} \cdot \mathbf{R}_{\kappa l}) \quad (13a)$$

and

$$F_{\kappa l}^{\alpha}(s) = q_{\alpha} F_0 \sin(\mathbf{q} \cdot \mathbf{R}_{\kappa l}), \quad (13b)$$

one can relate the quantities $E^c(\Omega, T)$ and $E^s(\Omega, T)$ [corresponding to Eq. (3)] to $S(\mathbf{q}, \omega)$ as

$$S(\mathbf{q}, \omega) \approx \frac{\langle n+1 \rangle}{\omega N} \frac{4\{E^c(\omega, T) + E^s(\omega, T)\}}{\pi T F_0^2}, \quad (14)$$

where $E^c(E^s)$ is obtained by substituting Eq. (13a) [(13b)] into Eq. (1).

Figure 3 shows the ω dependence of $S(\mathbf{q}, \omega)$ for five different \mathbf{q} along the $[100]$ direction. The number of sites is much larger than those in the works reported so far.⁷⁻¹⁰ The solid lines are only guides to the eye and the Bose factor is reduced. For small wave vector $q (< \xi^{-1})$, sharp peaks appear in the low-frequency region. With increasing $q = |\mathbf{q}|$, peak positions shift to the higher-frequency region beyond $\omega_c \approx 0.07$ and the widths (τ^{-1}) of the peaks increase very rapidly. This indicates that the linewidth of fracton is very broad, originating from the Ioffe-Regel strong scattering limit ($\tau^{-1} \approx \omega$).¹⁶

In this paper, we have performed large-scale computations for the Raman-scattering intensity $I_{\alpha\beta}(\omega)$ and the dynamical structure factor $S(\mathbf{q}, \omega)$ for $d=3$ bond-percolating networks. The numerical method we have used is very powerful to

obtain the insight into the dynamic correlation function. The ω dependences of the Raman-scattering intensities are calculated with the dipole-induced-dipole mechanism for $d=3$ percolation networks. For percolating networks at p_c , we have confirmed the validity of the scaling theory proposed by Alexander *et al.*,⁶ suggesting that the strain exponent takes the value $\sigma=0.97\pm 0.05$. We have also calculated the ω dependence of the Raman-scattering intensity for percolating networks above p_c . In the lower-frequency regime ($\omega < \omega_c$), our calculated results indicate clear phonon contribution. In the higher-frequency regime ($\omega > \omega_c$), the reduced Raman intensity has the same ω dependence as that for networks at the

percolation threshold p_c . We emphasize that the power-law dependence on frequency of $C_{\alpha\beta}(\omega)$, predicted theoretically for the system $p=p_c$,⁶ is valid for the system $p > p_c$. This supports the applicability of the scaling theory for the Raman-scattering intensity to actual systems such as silica aerogels.

This work was supported in part by a Grant-in-Aid from the Japan Ministry of Education, Science, and Culture (MESC). The authors thank the Supercomputer Center, Institute of Solid State Physics, University of Tokyo for the use of the facilities.

¹See for example, *Amorphous Solids*, edited by W. A. Phillips (Springer, Berlin, 1981).

²S. Alexander and R. Orbach, *J. Phys. (Paris)* **43**, L625 (1982).

³For a review, see T. Nakayama, K. Yakubo, and R. L. Orbach, *Rev. Mod. Phys.* **66**, 381 (1994).

⁴Y. Tsujimi, E. Courtens, J. Pelous, and R. Vacher, *Phys. Rev. Lett.* **60**, 2757 (1988).

⁵T. Nakayama, K. Yakubo, and R. Orbach, *J. Phys. Soc. Jpn.* **58**, 1891 (1989).

⁶S. Alexander, E. Courtens, and R. Vacher, *Physica A* **195**, 286 (1993).

⁷E. Stoll, M. Kolb, and E. Courtens, *Phys. Rev. Lett.* **68**, 2472 (1992).

⁸T. Nakayama and K. Yakubo, *J. Phys. Soc. Jpn.* **61**, 2601 (1992).

⁹M. Montagna, O. Pilla, G. Viliiani, V. Mazzacurati, G. Ruocco, and G. Signorelli, *Phys. Rev. Lett.* **65**, 1136 (1990).

¹⁰V. Mazzacurati, M. Montagna, O. Pilla, G. Viliiani, G. Ruocco, and G. Signorelli, *Phys. Rev. B* **45**, 2126 (1992).

¹¹M. L. Williams and H. J. Maris, *Phys. Rev. B* **31**, 4508 (1985).

¹²K. Yakubo, T. Nakayama, and H. J. Maris, *J. Phys. Soc. Jpn.* **60**, 3249 (1991).

¹³T. Terao, K. Yakubo, and T. Nakayama, *Phys. Rev. E* **50**, 566 (1994).

¹⁴For a review see T. Nakayama, in *Computational Physics as a New Frontier in Condensed Matter Research*, edited by H. Takayama *et al.* (The Physical Society of Japan, Tokyo, 1995), p. 21.

¹⁵W. Marshall and S. W. Lovesey, *Theory of Thermal Neutron Scattering* (Oxford University, Oxford, 1971).

¹⁶A. Aharony, S. Alexander, Ora Entin-Wohlman, and R. Orbach, *Phys. Rev. Lett.* **58**, 132 (1987).